Wavelet approximations of the Hamiltonian operator and computation of related energies

Claire Chauvin, Valérie Perrier

Wavelet approximations of the Hamiltonian operator and computation of related energies

Claire Chauvin * and Valérie Perrier †

February 2, 2008

Abstract

Multiresolution analysis in Quantum Chemistry provide efficient computational methods. In this article, we propose several representations of the Hamiltonian operator arising from the Density Functional Theory, based on orthogonal and interpolating scaling function bases. These high order approximations allows to compute the potential and kinetic energies with a linear complexity. Finally numerical examples show the accuracy of the method.

Keywords: Density Functional Theory, Orbital energy, Interpolating scaling function, $O(N)$ method, Stiffness Matrix, Harmonic Oscillator, Hydrogen.

Introduction

Ab initio molecular dynamics [25] provides a large class of methods for the Electronic structure calculations in quantum Chemistry. In this framework, we will focus on the Hohenberg-Kohn-Sham density functional theory, which leads to the resolution of nonlinear partial differential equations. In quantum chemistry two types of methods have been widely used: on the one hand, Slater-type or Gaussian-type basis decompositions for the solution use basis functions localized in physical space, generally centered at the center of nuclei and well adapted to the structure of the solution. On the other hand, the plane waves method involves functions localized in Fourier space but "delocalized" in physical space which does not favor the non uniform

*Laboratoire des Champs Magnétiques Intenses, CNRS Grenoble, France *Claire.Chauvin@grenoble.cnrs.fr*

†Laboratoire Jean Kuntzmann, Grenoble university and CNRS, France. *Valerie.Perrier@imag.fr*

structure of the solution. The advantage of this second method lies in the easy evaluation of operators and on the low computational complexity provided by the FFT. In between these two methods, wavelets appear as a good compromise between physical and Fourier representations. Like plane waves, wavelet decompositions are computed by a fast algorithm, the fast wavelet transform (FWT) being of linear complexity, and they provide polynomial approximations of arbitrary order [9].

For these reasons, wavelet methods have been introduced for electronic calculations [31, 8, 2, 18, 32, 30]. Moreover, the interpolation property of some wavelet families seems to be crucial for the treatment of the potential operator [15, 23, 1, 14, 16]. Indeed, the potential operator is usually represented in numerical works by its values on a grid.

The objective of this article is to present an efficient and accurate method for the computation of energies related to the Kohn-Sham operator. Classical error estimates are not available here because of the non elliptic form of the Hamiltonian, and because of its nonlinearity. On the other hand error estimates may be done in terms of energies (e.g. eigenvalues). We will focus in this article on numerical methods based on scaling functions, since it is the first step towards adaptive algorithms based on wavelets. Our method is firstly defined for the Kohn-Sham operator, and is based on the combination of interpolating scaling functions for the decomposition of the potential, and orthonormal scaling functions for the decomposition of the orbitals. Then the accuracy of the method is studied in the linear case, when the potential is reduced to the external potential: we derive error estimates for both the kinetic and potential energies. Finally, numerical tests on the simple models of Hydrogen and Harmonic Oscillator illustrate the efficiency of this approach.

1 Density Functional Theory

1.1 Kohn-Sham Equations

We present below the set of equations coming from the Density Functional Theory of Hohenberg, Kohn and Sham [20, 22]. Given K nuclei (positioned at $\mathbf{R}_\alpha$, $\alpha = 1, N$) and $2N$ electrons occupying N_o energy levels, the aim is to compute the electron density ρ, defined as:

$$\rho = 2 \sum_{i=1}^{N_o} n_i \, |u_i|^2, \quad \sum_{i=1}^{N_o} n_i = N, \quad 0 \leqslant n_i \leqslant 1,$$

where the occupied orbitals u_i satisfy the orthogonality relation $\int_\Omega u_i\, u_j\, d\mathbf{r} = \delta_{i,j}$, and are the N lowest eigenfunctions of the Kohn-Sham operator:

$$\begin{aligned} \mathcal{H}[\rho]\, u_i &= \epsilon_i\, u_i, \qquad i = 1, \ldots, N, & (1)\\ \mathcal{H}[\rho] &= -\frac{1}{2}\Delta + V(\mathbf{r}) + V_C[\rho] + V_{xc}[\rho] = -\frac{1}{2}\Delta + V_{KS}(\mathbf{r}). & (2) \end{aligned}$$

For simplicity we assume that $n_i = 1, \forall\, i = 1, \ldots, N_o$, and that the number of occupied energy levels N_o is equal to N. The external potential V and the Coulomb potential V_C describe respectively the attraction of the electron to the nuclei, and the Coulomb interaction between electrons:

$$\begin{aligned} V(\mathbf{r}) &= -\sum_{\alpha=1}^{K} \frac{Z_\alpha}{|\mathbf{r} - \mathbf{R}_\alpha|},\\ -\Delta V_C &= 4\pi\rho. \end{aligned}$$

The exchange-correlation potential V_{xc} in the Hamiltonian operator (2) is often evaluated by the Local Density Approximation (LDA) [25, 19]: V_{xc} depends only on the electron density $\rho(\mathbf{r})$.

Several iterative algorithms have been developed to solve this nonlinear system. The simplest one is called the Roothaan algorithm [29], and behaves like a fixed-point algorithm on the density ρ. Without going into details, the main idea is that for a given ρ, one is able to evaluate V_{KS}, and then to solve (1) by determining the lowest eigenvalues ϵ_i and corresponding eigenfunctions u_i. The existence of solution of such algorithms can be found in the literature [6, 4, 5, 30].

1.2 The model problem

An important step of the resolution of the self-consistent problem (1)–(2) is the determination of the lowest eigenvalues ϵ_i of a given Hamiltonian $\mathcal{H} = -\frac{1}{2}\Delta + V$, and of the corresponding eigenvectors u_i. At first, V is a function $V(\mathbf{r})$, and we focus on *a priori* estimates of approximate solutions of the linear problem in specific finite dimensional spaces.

Some results on the existence of a discrete spectrum are present in the literature [12, 28], with some condition on V. A first example is given by $V(\mathbf{r}) = \frac{K}{|\mathbf{r}|}$ with $K < 0$ in $\mathbb{R}^3$; in this case the spectrum of $\mathcal{H}$ is decomposed into a continuous part ($[0, +\infty[$) and a discrete part, which is minored by some $\epsilon \in \mathbb{R}$:

$$\epsilon < \epsilon_1 \leq \epsilon_2 \leq \cdots \leq \epsilon_m \leq \cdots < 0,$$

with possibly $\epsilon_i = \epsilon_{i+1} = \cdots = \epsilon_{i+m}$, e.g. eigenvalues with finite multiplicity. The corresponding eigenvectors are orthonormal in $L^2(\mathbb{R}^3)$.
Another example is given by the spectrum of the Harmonic Oscillator $\mathcal{H} = -\frac{1}{2}\Delta + \frac{1}{2}|\mathbf{r}|^2$ in $\mathbb{R}^3$ which is totally discrete, and composed of positive eigenvalues.

The weak formulation of problem (1-2) is the following:

$$\textit{Find } u_i \in H^1(\Omega), i = 1, \ldots, N, \textit{ such that:}$$

$$\frac{1}{2}\int_\Omega \nabla u_i \nabla v + < V\ u_i, v >= \epsilon_i < u_i,\ v >, \quad \forall\ v \in H^1(\Omega), \tag{3}$$

where $< u_i,\ v >= \int_\Omega u_i\ v$. These solutions u_i will be approximated in finite dimensional spaces presented in the next section. The convergence of discrete solutions towards continuous ones has been studied in the case of finite element methods, as explained in [28]. In the restrictive case where $\mathcal{H}$ is an elliptic operator, its approximate eigenvalues $\tilde{\epsilon}_i$ satisfy the following estimate:

$$|\epsilon_i - \tilde{\epsilon}_i| \leq C\ h^{2(m-1)}, \tag{4}$$

assuming suitable conditions on the approximation spaces, and that the i-first eigenvectors $(u_1, \cdots, u_i)$ belong to $H^m(\Omega)$ (h denotes the subdivision length). When ϵ_i is an eigenvalue of multiplicity 1, we also get:

$$\|u_i - \widetilde{u}_i\|_{H^1} \leq C\ h^{m-1}, \tag{5}$$

which means that the precision order in the eigenvalue approximation is twice better than the one obtained for the eigenvector in energy norm.

The aim of this paper is to study *a priori* estimates on the evaluation of the following energies:

$$\begin{aligned} \epsilon_i = \frac{< u_i,\ \mathcal{H}\ u_i >}{< u_i,\ u_i >} &= \frac{1}{2}\int_\Omega \nabla u_i \nabla v + < V\ u_i, u_i > \\ &= e_{kin} + e_p, \end{aligned} \tag{6}$$

where e_{kin} stands for the kinetic energy. We also search for a representation of $\mathcal{H}$ into suitable finite dimensional spaces, which will improve the efficiency of the calculation of the potential energy e_p .
The eigenvectors of $\mathcal{H}$ are known to have a polynomial decay when $|\mathbf{r}| \to +\infty$, we will thus study them in a domain that contains their support. Moreover, assuming that this domain is big enough, u_i vanish far from the boundaries, and we can consider periodic boundary conditions. Numerical advantages of

this choice are shown in next section.
The resolution scheme will depend on the representation of V_{xc} (2). Indeed in LDA, V_{xc} is evaluated from the grid values of ρ. Our choice is to expand ρ and the potential V into an interpolating scaling function basis. On the contrary, the orbitals u_i will be expanded into an orthonormal scaling functions basis, to take advantage of the nearly diagonalisation of elliptic operators, provided by the wavelet decomposition.

The next section will detail the finite dimensional spaces that will be used, generated by orthogonal or interpolating scaling function bases.

2 3D periodic Multiresolution Analysis (MRA)

Let $\omega = \mathbb{R}/\mathbb{Z}$ be the unit torus on $\mathbb{R}$, and $\Omega = (\mathbb{R}/\mathbb{Z})^3$. We first recall some basic properties of 3D periodic MRA in a general context. Then we will focus on orthonormal and interpolating scaling functions.

2.1 Construction

For more details on practical computations related to these bases, we refer to [11, 24]. A periodic MRA $\{\mathbb{V}_J\}$ of $L^2(\Omega)$ is constructed by an isotropic tensor product of one-dimensional MRA's $\{V_J\}$.

Notation 1 (MRA of $L^2(\omega)$) *Let $\{V_J\}$ and $\{\widetilde{V}_J\}$, $J \geqslant 0$ be the ascending dense sequences of two biorthogonal MRA's of $L^2(\omega)$. In the periodic case, the scaling functions $\phi_{J,k}$ and $\widetilde{\phi}_{J,k}$ which span the spaces*

$$V_J = span\{\phi_{J,k} \ ; \ k \in \omega_J = [0, \ldots, 2^J - 1]\} \quad \text{and} \quad \widetilde{V}_J = span\{\widetilde{\phi_{J,k}} \ ; \ k \in \omega_J\}$$

are generated by dilation, shift and periodization of scaling functions ϕ and $\widetilde{\phi}$ defined on $\mathbb{R}$:

$$\phi_{J,k}(x) = \sum_{r \in \mathbb{Z}} \phi(2^J(x+r) - k) \quad , \quad \widetilde{\phi}_{J,k}(x) = 2^J \sum_{r \in \mathbb{Z}} \widetilde{\phi}(2^J(x+r) - k).$$

Moreover, they satisfy the biorthogonality relation:

$$\int_\omega \phi_{J,k}(x) \ \widetilde{\phi}_{J,l}(x) \ dx = \delta_{k,l}, \quad \forall J \in \mathbb{N}, \quad \forall k, l \in \omega_J,$$

where $\delta_{k,l}$ is the Kronecker delta. The well-known two-scale equations rewrite in the periodic case:

$$\phi_{J,k} = \sum_{n \in \omega_{J+1}} h_{J+1}(n-2k)\ \phi_{J+1,n},$$
$$\widetilde{\phi}_{J,k} = \sum_{n \in \omega_{J+1}} \widetilde{h}_{J+1}(n-2k)\ \widetilde{\phi}_{J+1,n}. \tag{7}$$

where h_J and $\widetilde{h}_J$ are the filters coming from the 2^J-periodization of the filters h and $\tilde{h}$ associated to the scaling functions ϕ and $\widetilde{\phi}$.

We will assume that the scaling functions ϕ and $\tilde{\phi}$ have a compact support; this is equivalent to the fact that filters h_J and $\widetilde{h}_J$ have finite length. If the restrictions to $[0,1]$ of polynomials of degree less or equal than $m-1$ are contained in V_J, then the MRA $\{V_J\}$ is of approximation order m [9]. In this case, if we note P_{V_J} the biorthogonal projection into the space V_J:

$$\forall u \in L^2(\omega), \quad P_{V_J} u = \sum_{k \in \omega_J} < u / \widetilde{\phi}_{J,k} > \phi_{J,k},$$

then the following estimate holds:

$$\|u - P_{V_J} u\|_{H^s} \quad \lesssim \quad 2^{-J(m-s)}\ \|u\|_{H^m} \quad , \quad \forall\ u \in H^m(\omega) \tag{8}$$

Since our objective is the evaluation of the Kohn-Sham operator expanded into a scaling function basis, we will not introduce here wavelets. But the results presented in this article with scaling function bases, are also valid by using wavelets.
The construction of three-dimensional MRA is done as follows.

Definition 1 (MRA of $L^2(\Omega)$) *A couple of biorthogonal periodic MRA $\{\mathbb{V}_J\}$ and $\{\widetilde{\mathbb{V}}_J\}$ of $L^2(\Omega)$ is defined by isotropic tensor products of one-dimensional MRA's $\{V_J\}$ and $\{\widetilde{V}_J\}$:*

$$\mathbb{V}_J = V_J \otimes V_J \otimes V_J, \quad \text{and} \quad \widetilde{\mathbb{V}}_J = \widetilde{V}_J \otimes \widetilde{V}_J \otimes \widetilde{V}_J.$$

Let $\Omega_J = \omega_J^3$. A scaling function of $\mathbb{V}_J$ indexed by $\mathbf{k} = (k_1, k_2, k_3) \in \Omega_J$ writes for each $\mathbf{r} = (x, y, z) \in \Omega$:

$$\Phi_{J,\mathbf{k}}(\mathbf{r}) = \phi_{J,k_1}(x)\ \phi_{J,k_2}(y)\ \phi_{J,k_3}(z).$$

In the following, it will be convenient to adopt a vector-type notation for the basis: $\mathcal{F}_J = \{\Phi_{J,\mathbf{k}}\}_{\mathbf{k}\in\Omega_J}$, $\widetilde{\mathcal{F}}_J = \{\widetilde{\Phi}_{J,\mathbf{k}}\}_{\mathbf{k}\in\Omega_J}$. A function u of $\mathbb{V}_J$ with coefficients $C = \{c_{J,\mathbf{k}}\}_{\mathbf{k}\in\Omega_J}$ will be written as:

$$u = C^T\mathcal{F}_J = \sum_{\mathbf{k}\in\Omega_J} < u,\ \widetilde{\Phi}_{J,\mathbf{k}} >\ \Phi_{J,\mathbf{k}}.$$

In the next part we will introduce two specific families of scaling functions, which will be used for the decomposition of the orbitals u_i and the potential V.

2.2 Orthonormal and interpolating MRA's

For computational reasons, the orbitals u_i in (1) are expanded into an *orthonormal* basis [11]. Let $\{\mathbb{V}_J^{\perp}\}$ be an orthonormal MRA of $L^2(\Omega)$, of order m_1. In numerical tests we will use the Daubechies family and the Coiflets

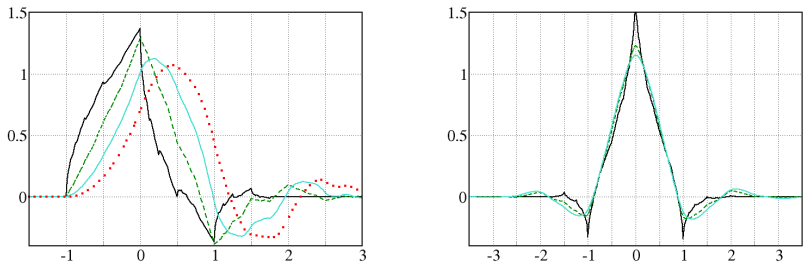

Figure 1: Left: Daubechies scaling functions of order from 2 (black line) to 5 (red dots). Right: Coifman scaling functions of order 2,4 and 6.

[11] (Fig.1). Daubechies wavelets are well suited to Electronic Structure Calculations [31, 17], because of their small compact supports related to their approximation properties. Observe on Fig.1 that Daubechies scaling functions are asymmetric. Coiflets are almost symmetric, but their supports are longer.

The potential will be expanded into a basis satisfying the interpolation property:

Definition 2 (Interpolating scaling function) *A 1D scaling function* θ

is interpolating if it satisfies the condition:

$$\theta(x-k) = \delta_{0,k} \quad , \quad \forall k \in \mathbb{Z}.$$

Let denote by $\mathbb{V}_J^c$ *a 3D interpolating MRA, generated by the 3D scaling functions:*

$$\Theta_{J,\mathbf{k}}(\mathbf{r}) = \Theta_{J,0}(x-\mathbf{k}) = \theta_{J,k_1}(x_1)\ \theta_{J,k_2}(x_2)\ \theta_{J,k_3}(x_3)$$

where $\theta_{J,k}(x) = \sum_{r\in\mathbb{Z}} \theta(2^J(x+r)-k)$ *has a* L^∞*-normalization. Therefore* $\Theta_{J,\mathbf{k}}$ *satisfies*

$$\Theta_{J,\mathbf{k}}(\frac{\mathbf{l}}{2^J}) = \delta_{\mathbf{k},\mathbf{l}}.$$

Such a function is also called Interpolet [13]. The biorthogonal scaling functions are given by $\widetilde{\Theta}_{J,\mathbf{k}}(.) = 2^{3J}\delta(2^J. - \mathbf{k})$. The approximation order of $\mathbb{V}_J^c$ will be called m_2. Interpolating scaling functions of several orders are shown on figure Fig.2.

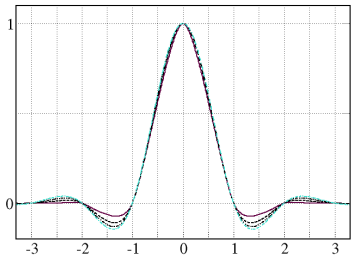

Figure 2: Interpolating scaling functions of orders 4,6,8,10. The oscillations increase with the order.

As explained in section 1, the potential V defined on Ω is known at grid points $\mathbf{k}/2^J$, $\mathbf{k} \in \Omega_J$. Let $\mathrm{V} = \{v_{J,\mathbf{k}}\}_{\mathbf{k}\in\Omega_J} = \{V(\mathbf{k}/2^J)\}_{\mathbf{k}\in\Omega_J}$ be the grid values, the interpolation of V into $\mathbb{V}_J^c$ is given by:

$$P_{V_J^c}V(\mathbf{r}) = \mathrm{V}_J(\mathbf{r}) = \mathrm{V}^T\mathcal{T}_J = \sum_{\mathbf{k}\in\Omega_J} v_{J,\mathbf{k}}\ \Theta_{J,\mathbf{k}}(\mathbf{r}) = \sum_{\mathbf{k}\in\Omega_J} < V, \widetilde{\Theta}_{J,\mathbf{k}} >\ \Theta_{J,\mathbf{k}}(\mathbf{r}) \tag{9}$$

with $\mathcal{T}_J = \{\Theta_{J,\mathbf{k}}\}_{\mathbf{k}\in\Omega_J}$. The objective now is to apply the operator V to an orbital u_i in an efficient way. This means to reduce as far as possible the computational cost, which can become huge in three dimensions.

3 Representation of the Hamiltonian operator

In this part we will assume that V depends only on the space variable $\mathbf{r}$. We first present estimates for the kinetic and potential energies in some cases. Then, we show that in the Galerkin formulation, the application of the potential operator to an orbital can have a high computational cost. One solution for this problem is to consider the projection operators onto the spaces introduced in section 2.

3.1 Galerkin formulation

We look for solutions $\widetilde{u}_i$ of system (3) in the space $\mathbb{V}_J^{\perp}$, given by their coefficients C_i in an orthonormal scaling function basis $\mathcal{F}_J = \{\Phi_{J,\mathbf{k}}\}_{\mathbf{k}\in\Omega_J}$:

$$\tilde{u}_i(\mathbf{r}) = C_i^T \mathcal{F}_J = \sum_{\mathbf{k}\in\Omega_J} c_{J,\mathbf{k}}^{(i)}\ \Phi_{J,\mathbf{k}}(\mathbf{r}), \tag{10}$$

with $C_i = \{c_{J,\mathbf{k}}^{(i)}\}_{\mathbf{k}\in\Omega_J}$. The system (3) is then reduced to:

$$\left[\mathbb{A} + {}^{G}\mathbb{B}\right] C_i = \epsilon_i\ C_i$$

where $\mathbb{A} = [\mathbb{A}_{\mathbf{k},\mathbf{k}'}]$ and ${}^{G}\mathbb{B} = [{}^{G}\mathbb{B}_{\mathbf{k},\mathbf{k}'}]$ are the following matrices (the exponent G stands for Galerkin):

$$\begin{aligned} \forall\ \mathbf{k},\mathbf{k}' \in \Omega_J \quad \mathbb{A}_{\mathbf{k},\mathbf{k}'} &= \frac{1}{2}\int_{\Omega} \nabla\Phi_{J,\mathbf{k}}\ \nabla\Phi_{J,\mathbf{k}'}, \\ {}^{G}\mathbb{B}_{\mathbf{k},\mathbf{k}'} &= <\Phi_{J,\mathbf{k}}, V_J\ \Phi_{J,\mathbf{k}'}>. \end{aligned}$$

We will focus now on the evaluation of the energies for one orbital. We thus abandon the index i, and call the approximated solution $\tilde{u}$. The orbitals $\tilde{u}$ are orthonormal in $\mathbb{V}_J^{\perp}$, which implies $C^T C = 1$. The total energy of $\tilde{u}$ is given by $\widetilde{\epsilon} = \widetilde{e}_{kin} + \widetilde{e}_p$, where $\widetilde{e}_{kin}$ stands for the kinetic energy and $\widetilde{e}_p$ for the potential energy.

Kinetic energy: the kinetic energy $\widetilde{e}_{kin}$ related to the approximate orbital $\tilde{u}$ is given by:

$$\widetilde{e}_{kin} = \frac{C^T\ \mathbb{A}\ C}{C^T\ C} = C^T\ \mathbb{A}\ C. \tag{11}$$

Then we have the well known result [28] in the particular case where the potential V is zero:

Proposition 1 *Let u be an orbital. Assume that u and all the orbitals of lower energy belong to $H^s(\Omega)$. Then the error between the kinetic energy e_{kin}, and the computed energy $\tilde{e}_{kin}$ behaves like:*

$$|e_{kin} - \tilde{e}_{kin}| \lesssim 2^{-2J(r_1-1)}, \tag{12}$$

with $r_1 = \min(s, m_1)$.

Potential energy: The potential energy related to an orbital u is given by:

$$e_p(u) =< u, Vu > .$$

In the Galerkin formulation, the potential energy of the approximate orbital $\tilde{u}$ is:

$$\tilde{e}_p =< \tilde{u},\ \mathrm{V}_J\ \tilde{u} >= \frac{C^T\ {}^G\mathbb{B}\ C}{C^T\ C} = C^T\ {}^G\mathbb{B}\ C. \tag{13}$$

Since the potential V is expanded into a finite dimensional interpolating scaling function basis $\{\Theta_{J,\mathbf{k}}\}$ (see (9)), an element of the potential Stiffness matrix ${}^G\mathbb{B}$ writes:

$$\begin{aligned} For\ \mathbf{k},\mathbf{k}' \in \Omega_J, \quad {}^G\mathbb{B}_{\mathbf{k},\mathbf{k}'} &= < \Phi_{J,\mathbf{k}}, \mathrm{V}_J\ \Phi_{J,\mathbf{k}'} > \\ &= \int_\Omega \Phi_{J,\mathbf{k}}(\mathbf{r})\ \mathrm{V}_J(\mathbf{r})\ \Phi_{J,\mathbf{k}'}(\mathbf{r})\ d\mathbf{r} \\ &= \sum_{\mathbf{m}\in\Omega_J} v_{J,\mathbf{m}} \int_\Omega \Phi_{J,\mathbf{k}}(\mathbf{r})\ \Theta_{J,\mathbf{m}}(\mathbf{r})\ \Phi_{J,\mathbf{k}'}(\mathbf{r})\ d\mathbf{r} \\ &= \sum_{\mathbf{m}\in\Omega_J} v_{J,\mathbf{m}}\ \mathbf{T_J}(\mathbf{k}-\mathbf{m}, \mathbf{k}'-\mathbf{m}), \end{aligned}$$

where $\mathbf{T_J}(\mathbf{k},\mathbf{k}') = \displaystyle\int_\Omega \Phi_{J,\mathbf{k}}(\mathbf{r})\ \Theta_{J,\mathbf{0}}(\mathbf{r})\ \Phi_{J,\mathbf{k}'}(\mathbf{r})\ d\mathbf{r}$. Since the basis functions are periodic tensor-product functions, each term $\mathbf{T_J}(\mathbf{k},\mathbf{k}')$ is a product of three cyclic matrices T, whose coefficients are called connection coefficients [10, 27]:

$$T(k,k') = \int_\omega \phi(x-k)\ \theta(x)\ \phi(x-k')\ dx.$$

Details of the calculation can be found in the thesis [7]. The mean idea is that, thanks to the symmetry around the function $\Theta_{J,\mathbf{m}}$, the calculation of ${}^G\mathbb{B}_{\mathbf{k},\mathbf{k}'}$ is obtained by a bidimensional convolution of coefficients V with elements of the matrix $\mathbf{T_J}$.

Suppose now that the Hamiltonian $\mathcal{H}$ is elliptic, for instance if V satisfies $\inf_{\mathbf{r}\in\mathbf{\Omega}} V(\mathbf{r}) > -\mathbf{1}$; then the exact and approximate orbitals fulfill the approximation error (using (5) and (8)):

$$\|u - \tilde{u}\| \leq C\ 2^{-Jr_1}\ \|u\|_{H^{r_1}} \tag{14}$$

with $r_1 = \min(s, m_1)$. In this case, we may derive the following error estimate.

Proposition 2 *Let u be an orbital. Assume that u and all the orbitals of lower energy belong to $H^s(\Omega)$. Suppose also that the potential $V \in H^L(\Omega)$. Then the error between the exact potential energy $e_p(u)$ and the approximate potential energy $\tilde{e}_p(\tilde{u})$ behaves like:*

$$|e_p(u) - \tilde{e}_p(\tilde{u})| \lesssim C_1\ 2^{-Jr_1} + C_2\ 2^{-Jr_2}, \tag{15}$$

with $r_1 = \min(s, m_1)$, $r_2 = \min(L, m_2)$.

Proof:

$$\begin{aligned} |e_p(u) - \tilde{e}_p(\tilde{u})| &= |e_p(u) - e_p(\tilde{u}) + e_p(\tilde{u}) - \tilde{e}_p(\tilde{u})| \\ &\leqslant \left|\int_\Omega V\ (u^2 - \tilde{u}^2)\right| + \left|\int_\Omega (V - \mathrm{V}_J)\ \tilde{u}^2\right| \end{aligned}$$

Using (14) yields:

$$\begin{aligned} \left|\int_\Omega V\ (u^2 - \tilde{u}^2)\right| &\leqslant \|V\|_{L^\infty}\ \int_\Omega |(u - \tilde{u})(u + \tilde{u})| \\ &\lesssim 2\ \|V\|_{L^\infty}\ \|u\|\ \|u - \tilde{u}\| \\ &\lesssim 2^{-Jr_1}\ \|V\|_{L^\infty}\ \ \|u\|\ \|u\|_{H^{r_1}}. \end{aligned}$$

The second term can be majored by:

$$\begin{aligned} \left|\int_\Omega (V - \mathrm{V}_J)\ \tilde{u}^2\right| &\lesssim \|V - \mathrm{V}_J\|_{L^\infty}\ \|u\|^2 \\ &\lesssim 2^{-Jr_2}\ \|V\|_{H^{r_2}}\ \|u\|^2 \end{aligned}$$

with $r_2 = \min(L, m_2)$, using classical interpolation error. We thus get the estimate (15).

Table 1: Number of coefficients of $\mathbf{T_J}$ located between two magnitudes, with $m_1 = 2$ and $m_2 = 8$. For example 9420 is the number of coefficients greater in absolute value than 10^{-8}, and smaller than 10^{-4}.

$\lvert\mathbf{T_J}(\mathbf{k},\mathbf{k}')\rvert$	$> 10^{-4} >$	$> 10^{-8} >$	$> 10^{-11}$
#	684	9420	14980

Drawbacks The evaluation of $\mathbf{T_J}$ is expensive in terms of computational cost, as already mentioned in [26]. For $m_1 = 4$ (Daubechies) and $m_2 = 8$ (Interpolet), T has almost 30 coefficients greater than 10^{-8}. In three dimensions, Table 1 shows the repartition of the coefficient size. Obviously, the coefficients are localized near the diagonal (for $\mathbf{k}$ close to $\mathbf{k}'$).

Several work have been done to overcome this complexity, based on quadrature formula [21, 26]. More particularly, Neelov and Goedecker [26] use quadrature formula with an exactness order linked to scaling function order. They showed that the quadratic order for the error convergence was respected both in uniform and non uniform grid, in one dimension.

3.2 Biorthogonal Projection operators

We present now the projectors associated to the three types of scaling function basis (orthonormal basis, interpolation basis and its biorthogonal one).

Notation 2 (Orthogonal projector $P_{V_J^\perp}$) *Let $P_{V_J^\perp}$ be the orthogonal projection of $L^2(\Omega)$ into $\mathbb{V}_J^\perp$:*

$$P_{V_J^\perp} : \left\{ \begin{array}{lll} L^2(\Omega) & \longmapsto \mathbb{V}_J^\perp, & \\ u & \longrightarrow P_{V_J^\perp} u & = \sum_{\mathbf{k}\in\Omega_J} < u, \Phi_{J,\mathbf{k}} > \Phi_{J,\mathbf{k}}. \end{array} \right.$$

Notation 3 (Interpolation operator $P_{V_J^c}$) *Let $P_{V_J^c}$ be the interpolation operator of $C^0(\Omega)$ into $\mathbb{V}_J^c$:*

$$P_{V_J^c} : \left\{ \begin{array}{lll} C^0(\Omega) & \longmapsto \mathbb{V}_J^c, & \\ u & \longrightarrow P_{V_J^c} u & = \sum_{\mathbf{k}\in\Omega_J} < u, \widetilde{\Theta}_{J,\mathbf{k}} > \Theta_{J,\mathbf{k}} = \sum_{\mathbf{k}\in\Omega_J} u_{J,\mathbf{k}} \Theta_{J,\mathbf{k}}. \end{array} \right.$$

Notation 4 (Biorthogonal projection $P_{\widetilde{V}_J^c}$) *Let $P_{\widetilde{V}_J^c}$ be the projector of $L^2(\Omega)$ into $\widetilde{\mathbb{V}}_J^c$ ($\subset H^{-1}(\Omega)$):*

$$P_{\widetilde{V}_J^c} : \left\{ \begin{array}{ccc} L^2(\Omega) & \longmapsto \widetilde{\mathbb{V}}_J^c, & \\ u & \longrightarrow P_{\widetilde{V}_J^c} u & = \displaystyle\sum_{\mathbf{k}\in\Omega_J} < u, \Theta_{J,\mathbf{k}} > \widetilde{\Theta}_{J,\mathbf{k}}. \end{array} \right.$$

Following [9] and [3], the projectors $P_{V_J^\perp}$ and $P_{V_J^c}$ satisfy the error estimate (8): if m_1 (resp. m_2) is the approximation order of $\mathbb{V}_J^\perp$ (resp. $\mathbb{V}_J^c$), then the errors in L^2-norm between a function $u \in H^s(\Omega)$ and its projections behave as:

$$\|u - P_{V_J^\perp} u\| \lesssim 2^{-Jr_1} \|u\|_{H^{r_1}}, \quad r_1 = \min(m_1, s), \tag{16}$$

$$\|u - P_{V_J^c} u\| \lesssim 2^{-Jr_2} \|u\|_{H^{r_2}}, \quad r_2 = \min(m_2, s). \tag{17}$$

Such an estimate is quite different in case of the third operator $P_{\widetilde{V}_J^c}$. As $\widetilde{\mathbb{V}}_J^c$ is spanned by Delta-functions, the projection $P_{\widetilde{V}_J^c} u$ of a given function u leaves in the Sobolev space H^{-1} of negative exponent, endowed by the H^{-1}-norm:

$$\forall\ u \in H^{-1}, \quad \|u\|_{H^{-1}} = \sup_{\substack{\phi \in H^1(\Omega) \\ \|\phi\|_{H^1} = 1}} | < u,\ \phi >_{H^{-1},H^1} |.$$

In this context, the following error estimate can be proved, following [**?**]:

Proposition 3 *The projection error of a L^2-function u, provided by $P_{\widetilde{V}_J^c}$, behaves in the space H^{-1} as:*

$$\|u - P_{\widetilde{V}_J^c} u\|_{H^{-1}} \lesssim 2^{-J(r_2+1)} \|u\|_{H^{r_2}}. \tag{18}$$

if r_2??.

Remark 1 *There exists several ways to define a projector $P_{V_J^c}$, since there exist several biorthogonal spaces $\widetilde{\mathbb{V}}_J^c$ associated to the primal space $\mathbb{V}_J^c$. Notice also that for $u \in \mathbb{V}_J^\perp$, $P_{V_J^\perp} P_{V_J^c} u \neq u$ in general.*

Practical use of projectors Numerically, these projectors are applied to functions of the finite dimensional spaces $\mathbb{V}_J^{\perp}$, $\mathbb{V}_J^c$, or $\widetilde{\mathbb{V}}_J^c$, spanned by the respective bases $\mathcal{F}_J$, $\mathcal{T}_J$ and $\widetilde{\mathcal{T}}_J$. These projectors are entirely defined by the following matrices Z, X and $Y \in \mathcal{M}_J$, where $\mathcal{M}_J$ is the set of $2^{3J} \times 2^{3J}$ real valued matrices.

Notation 5

$$P_{V_J^{\perp}} : \left\{ \begin{array}{ccc} \mathbb{V}_J^c & \longmapsto & \mathbb{V}_J^{\perp}, \\ u = D^T \mathcal{T}_J & \stackrel{Z}{\longrightarrow} & P_{V_J^{\perp}} u = (ZD)^T \mathcal{F}_J = C^T \mathcal{F}_J, \end{array} \right.$$

where $Z =< \mathcal{T}_J, \mathcal{F}_J >= \left\{ < \Theta_{J,\mathbf{k}}, \Phi_{J,\mathbf{k}'} > \right\}_{\mathbf{k},\mathbf{k}' \in \Omega_J}$.

$$P_{V_J^c} : \left\{ \begin{array}{ccc} \mathbb{V}_J^{\perp} & \longmapsto & \mathbb{V}_J^c, \\ u = C^T \mathcal{F}_J & \stackrel{X}{\longrightarrow} & P_{V_J^c} u = (XC)^T \mathcal{T}_J = D^T \mathcal{T}_J, \end{array} \right.$$

where $X =< \mathcal{F}_J, \widetilde{\mathcal{T}}_J >= \left\{ < \Phi_{J,\mathbf{k}}, \widetilde{\Theta}_{J,\mathbf{k}'} > \right\}_{\mathbf{k},\mathbf{k}' \in \Omega_J}$.

$$P_{\widetilde{V}_J^c} : \left\{ \begin{array}{ccc} \mathbb{V}_J^{\perp} & \longmapsto & \widetilde{\mathbb{V}}_J^c, \\ u = C^T \mathcal{F}_J & \stackrel{Z^T}{\longrightarrow} & P_{\widetilde{V}_J^c} u = (Z^T C)^T \widetilde{\mathcal{T}}_J = \widetilde{D}^T \widetilde{\mathcal{T}}_J. \\ \mathbb{V}_J^c & \longmapsto & \widetilde{\mathbb{V}}_J^c, \\ u = D^T \mathcal{T}_J & \stackrel{Y}{\longrightarrow} & P_{\widetilde{V}_J^c} u = (YD)^T \widetilde{\mathcal{T}}_J = \widetilde{D}^T \widetilde{\mathcal{T}}_J. \end{array} \right.$$

where $Y =< \mathcal{T}_J, \mathcal{T}_J >= \left\{ < \Theta_{J,\mathbf{k}}, \Theta_{J,\mathbf{k}'} > \right\}_{\mathbf{k},\mathbf{k}' \in \Omega_J}$.

Applying Z, X or Y to a set of 2^{3J} coefficients is easily done by three successive one-dimensional convolutions [7]. Using such technique in potential energy evaluation can thus improve significantly the complexity. Indeed, applying the matrix Z to a set of 2^{3J} coefficients costs $3(l_1 + l_2 - 1)2^{3J}$, with l_1 and l_2 the support lengths of the 1D scaling functions ϕ and θ. Applying X costs $3\ l_1\ 2^{3J}$, since the filter corresponding to $\widetilde{\theta}$ is $\delta_{0,k}$.
The main difference with the method used in [26] is that we can approximate the coefficients C for the expansion in $\mathbb{V}_J^{\perp}$ with an order independent of m_1. In [26], the best order of approximation of $< u,\ \Phi_{J,\mathbf{k}} >$ is $2m_1$, whereas in our method we first project $u \in L^2(\Omega)$ in $\mathbb{V}_J^c$ of any order m_2, and then project into $\mathbb{V}_J^{\perp}$. Moreover, the cost per grid point is in our case $3(l_1 + l_2 - 1)$, and in their case $3(2\ l_1 + 3)$. If l_1 and l_2 are equal, then both methods are similar. The numerical studies of section 4 gives the estimations of a good choice of m_1 and m_2, according to the following approximation inequalities.

Approximation error of successive transfers to different MRA

Lemma 1 *Let $u \in H^s(\Omega)$, m_1 be the order of $\mathbb{V}_J^{\perp}$, and m_2 the order of $\mathbb{V}_J^c$. Successive projections onto $\mathbb{V}_J^{\perp}$ and $\mathbb{V}_J^c$ of u provide the following estimates:*

$$\|u - P_{V_J^c} P_{V_J^{\perp}} u\|_{L^2} \lesssim 2^{-Jr_1} \ \|u\|_{H^{r_1}} + 2^{-Jr_2} \ \|u\|_{H^{r_2}}. \tag{19}$$

with $r_1 = min(m_1, m_2)$ and $r_2 = min(s, m_1)$.

In the same way, the transfer through $\widetilde{\mathbb{V}}_J^c$ and $\mathbb{V}_J^{\perp}$ leads to:

$$\|u - P_{\widetilde{V}_J^c} P_{V_J^{\perp}} u\|_{H^{-1}} \lesssim 2^{-J(r_1+1)} \ \|u\|_{H^{r_1}} + 2^{-J(r_2+1)} \ \|u\|_{H^{r_2}}. \tag{20}$$

The proof of the estimates (19) and (20) comes simply using the triangular inequality and estimations (16), (17) and (18).

The following example is an illustration of lemma 1 with a smooth function.

Example 1 *Let u be a Gaussian function discretized on an interpolating basis, with coefficient vector D. As $u \in H^s(\Omega)$ for all $s > 0$, only the orders m_1 of $\mathbb{V}_J^{\perp}$ and m_2 of $\mathbb{V}_J^c$ interfere in convergence rates.*

(1) Do successive passage to $\mathbb{V}_J^c$ and $\mathbb{V}_J^{\perp}$, by applying the matrix ZX. Then evaluate the error $||D - (XZ)^n D||_{l_2}$. According to (19), the approximation follows the law $2^{-J \min(m_1,\ m_2)}$.

(2) Second, apply n times $Z^T Z$ to C, then compute the error $||D - (Z^T Z)^n D||_{l_2}$. The projection of $P_{\widetilde{V}_J^c} P_{V_J^{\perp}} f$ to $\mathbb{V}_J^c$ is done by applying the Identity matrix, since $\mathbb{V}_J^c$ and $\widetilde{\mathbb{V}}_J^c$ are biorthogonal.

The results are shown in figure Fig.3 and in table TAB[1] . For one couple $(\mathbb{V}_J^{\perp}, \mathbb{V}_J^c)$, two curves are plotted: they correspond to the convergence order of the curves shown in figure Fig.3, evaluated by a least square procedure.

In the method (1), the convergence orders correspond rather good to the competition of r_1 and r_2 shown in the a priori *estimate (19).*

For the method (2), we have also evaluated the error in L^2 norm: the convergence errors are better than in method (1), which is not predicted by (20).

3.3 Application to the computation of energies

The application of the Hamiltonian operator (2) to an orbital u has two parts:
1) apply a derivation filter (kinetic part),
2) multiply by the real function V (potential part). In this part, we will introduce approximations $\tilde{u}$ of the orbital u (10).

Table 2: Error rates for several $\mathbb{V}_J^{\perp}$ and $\mathbb{V}_J^c$.

D3 I8		D4 I6		D4 I10		D5 I6		D4 C2		D4 C6	
3.03	6.08	3.94	5.96	3.76	7.83	5.78	6.33	3.42	3.87	3.70	7.46

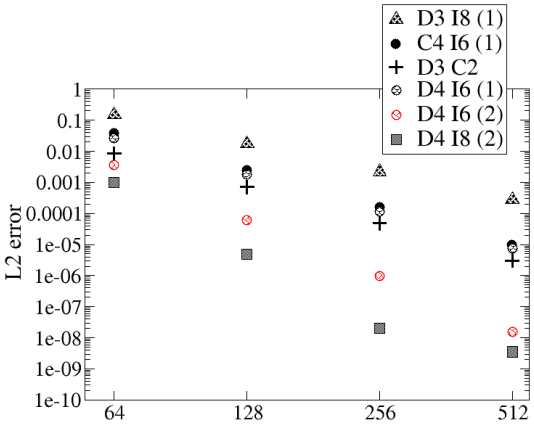

Figure 3: Errors (1) $||D-(XZ)^n D||_{l_2}$ and (2) $||D-(Z^TZ)^n D||_{l_2}$ for several 2^J, with $n=10$. The legend corresponds to couples ($\mathbb{V}_J^{\perp}$, $\mathbb{V}_J^c$) of orders m_1 and m_2. D stands for Daubechies, C for Coiflet and I for interpolet families.

3.3.1 Kinetic energy

To the kinetic energy (11) we associate the relative error τ_{kin}:

$$\widetilde{e}_{kin} = \frac{C^T \, \mathbb{A} \, C}{C^T \, C}, \quad \text{and} \quad \tau_{kin} = \frac{|e_{kin} - \widetilde{e}_{kin}|}{|e_{kin}|}.$$

3.3.2 Potential Energy

We construct now two representations of the Hamiltonian operator: we start from the potential V_J expanded in the collocation basis $\mathcal{T}_J$ Eq. (9) and we will deduce two expressions for the approximate potential energy $\widetilde{e}_p$. To that purpose, we will define two kinds of matrix-matrix product and matrix-vector product:

Notation 6 (Matrix-matrix and matrix-vector products) *Let two real*

matrices A and $B \in \mathcal{M}_J$ of size $2^{3J} \times 2^{3J}$, and two vectors U and V of size 2^{3J} be given. The standard matrix-matrix product writes $A\ B$, whereas the standard matrix-vector product writes $A\ U$. On the other hand, the matrix-matrix product $\cdot$, and the matrix-vector product $\cdot$ will denote an element-by-element multiplication, as follows:

$$\begin{aligned}(U \cdot A)_{ij} &= U_i A_{ij}, \\ (U \cdot V)_i &= u_i v_i.\end{aligned}$$

Method 1 The bilinear form associated to V_J is written in $\mathbb{V}_J^{\perp} \times \mathbb{V}_J^{\perp}$:

$$< u,\ V\ v > \ \sim \ < u,\ P_{V_J^{\perp}}(\mathrm{V}_J P_{V_J^c}\ v) >, \quad \forall\ u, v \in \mathbb{V}_J^{\perp}.$$

and its representation in the basis $\mathcal{F}_J$ yields the Stiffness Matrix:

$$^1\mathbb{B} = \ Z\ (\mathrm{V} \cdot X).$$

If $D = X\ C$, that is if D is the collocation vector of u on $\mathbb{V}_J^c$, and if $\widetilde{D} = Z^T C$, where $\widetilde{D}$ corresponds to the coefficients of u in the dual interpolating basis, then the potential energy $^1\widetilde{e}_p$ is approximated by:

$$^1\widetilde{e}_p = \frac{\widetilde{D}^T\ (\mathrm{V} \cdot D)}{\widetilde{D}^T D}.$$

Method 2 We approximate the bilinear form associated to V_J by:

$$< u,\ V\ v > \ \sim \ < u, P_{V_J^{\perp}}\ P_{V_J^c}\ (\mathrm{V}_J\ P_{\widetilde{V}_J^c} v) >, \quad \forall\ u, v \in \mathbb{V}_J^{\perp}$$

Its matrix representation in the basis $\mathcal{F}_J$ and the potential energy of an element $u \in \mathbb{V}_J^{\perp}$ write:

$$^2\mathbb{B}^J = Z\ (\mathrm{V} \cdot Z^T),$$

$$^2\widetilde{e}_p = \frac{\widetilde{D}^T\ (\mathrm{V} \cdot \widetilde{D})}{\widetilde{D}^T \widetilde{D}}.$$

Next section presents the relative errors for the potential energy in the three cases: Galerkin, methods 1 and 2. The relative error writes:

$$^{G,1,2}\tau_p = \frac{|e_p - \ ^{G,1,2}\widetilde{e}_p|}{|e_p|}, \tag{21}$$

where e_p is the potential energy of the exact orbital u.

4 Numerical Applications

We have done three-dimensional tests on two linear Hamiltonian operators.

1. The Harmonic Oscillator: the potential V_o and the solution u_o are very regular, so that we can observe numerically the error estimates depending only on the basis order.

2. The Hydrogen atom: the potential V_h and the orbital u_h are both in $\mathcal{C}^0$, and leads to more complicated laws for the error behavior.

In the tests presented here, we have made a dilation of the space Ω: for all $\mathbf{r} = (X, Y, Z) \in \Omega$, we associate the triplet (x, y, z) such that $X = \frac{x}{L}$, $Y = \frac{y}{L}$, $Z = \frac{z}{L}$, with $L = 10$. The orbital u is expanded into the space $\mathbb{V}_J^c$ of interpolating scaling functions of order m_2:

$$P_{V_J^c} u = \sum_{\mathbf{k} \in \Omega_J} u(x_{J,\mathbf{k}})\ \Theta_{J,\mathbf{k}}. \tag{22}$$

Starting from Eq.(22), we evaluate $\widetilde{e}_{kin}$ and $\widetilde{e}_p$. The coefficients $C = \{c_{J,\mathbf{k}}\}_{\mathbf{k} \in \Omega_J}$ are obtained by applying a change of basis:

$$P_{V_J^\perp}\ u = \sum_{\mathbf{k} \in \Omega_J}\ c_{J,\mathbf{k}}\ \Phi_{J,\mathbf{k}} = C^T \mathcal{F}_J = (ZD)^T \mathcal{F}_J. \tag{23}$$

4.1 Harmonic oscillator

The model for the Harmonic Oscillator is:

$$\mathcal{H} = -\frac{1}{2}\Delta + \frac{1}{2}|\mathbf{r}|^2, \quad \mathbf{r} \in \Omega.$$

A solution $(\mathcal{E}_o,\ u_o)$ of the eigenproblem $\mathcal{H}u = \mathcal{E}u$ is known analytically:

$$\begin{aligned}
u_o(\mathbf{r}) &= C_N\ e^{-|\mathbf{r}|^2/2}, \quad \forall\ \mathbf{r} \in \Omega \\
\mathcal{E}_o &= e_{kin} + e_p, \\
e_{kin} &= \frac{< u_o| -\frac{1}{2}\Delta |u_o >}{< u_o|u_o >} = 0.75\ a.u., \\
e_p &= \frac{< u_o| \frac{1}{2}|\mathbf{r}|^2 |u_o >}{< u_o|u_o >} = 0.75\ a.u..
\end{aligned} \tag{24}$$

C_N is a normalization factor, based on the L^2 norm of u_o: $\|u_o\|_2 = 1$. The orbital u_o decays rapidly, so there is no need to have a great L. In this example, the orbital u_o and the potential V_o live in C^∞, then the convergence order depends only on the space approximation orders m_1 and m_2.

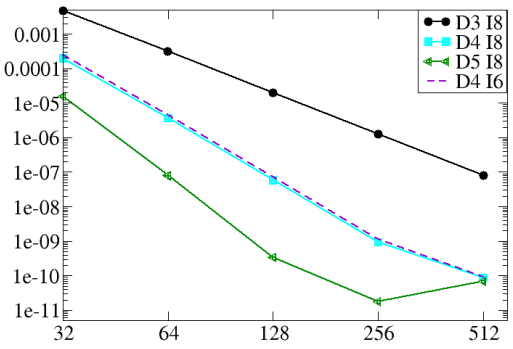

Figure 4: Harmonic Oscillator: relative error τ_{kin} as a function of 2^J. Different orders m_1 and m_2 are considered.

4.1.1 Kinetic energy

Fig.4 shows the behavior of the relative error τ_{kin} in terms of 2^J, on a log/log plot. Two Interpolet orders, $m_2 = 6$ and $m_2 = 8$, with an orthogonal order of $m_1 = 4$, are considered: the dependency on m_2 is weak. We obtain the following behavior for the relative error:

$$\tau_{kin} \sim C\ 2^{-2J(m_1-1)},$$

which can be seen as an extension of property (12). Indeed, this property holds for a pure Laplacian operator. Here, we have recovered this estimation for an eigenvector of the Hamiltonian associated to the Harmonic Oscillator, and its kinetic part.

Below 10^{-9}, the machine precision interferes with the values. The results are very similar for a Symmlet and a Daubechies scaling function of same order (the Stiffness matrices of the Laplacian are identical). We get the same result with Coiflets (the error is of order 10^{-5} for $2^J = 32$), but Daubechies functions have shorter support, and thus have more numerical interest.

The error between the exact and the approximated energy is thus quadratic as a function of J and m_1. Remember that if we want to get an energy with some precision ϵ, we only need a precision of $\sqrt{\epsilon}$ on the orbital.

4.1.2 Potential Energy

Galerkin formulation In case of Harmonic Oscillator, it is easy to evaluate the Galerkin Stiffness matrix, thanks to the separability properties of the operator and the solution:

$$\begin{aligned} V_o(\mathbf{r}) &= \frac{1}{2}(x^2+y^2+z^2) = v(x)+v(y)+v(z), \\ u_o(\mathbf{r}) &= C_N\ e^{-|\mathbf{r}|^2/2} = u(x)\ u(y)\ u(z), \\ u(x) &= C_N^{1/3} e^{-x^2/2}. \end{aligned}$$

Let $\omega = [0, L[$, we can express the potential energy in terms of the one dimensional quantity:

$$e_p = \int_\Omega u_o(\mathbf{r})\ V_o(\mathbf{r})\ u_o(\mathbf{r})\ d\mathbf{r} = 3\int_\omega v(x)\ u^2(x)\ dx = 3\times\frac{1}{4}.$$

	D4 I8	D3 I8	D3 I4
32	0.7500070985	0.750043907	0.75055975
64	0.750000030114	0.75000067514	0.750033937
128	0.750000000058755	0.750000010427	0.750000010427

Table 3: Harmonic Oscillator: potential energy ${}^G\tilde{e}_p$ in case of Galerkin formulation.

Table 3 shows the potential energies ${}^G\tilde{e}_p$ for different couples (m_1, m_2). As the solution is highly regular, the precision only depends on these two orders. The convergence rates are in these three cases 8.5, 6.2 and 4. This suggests an error behavior like:

$${}^G\tau_p \sim C\ 2^{-J\ \min(2m_1+\alpha,\ m_2)}, \qquad \alpha \leqslant \frac{1}{2}.$$

A reasonable choice is thus an Interpolet order $m_2 \geqslant 2m_1$.

Method 1 Figure Fig.5 shows the evolution of the relative error ${}^1\tau_p$ defined in Eq.(21) as a function of 2^J, for different couples (m_1, m_2). The coefficient rate behaves like:

$${}^1\tau_p \sim C_1\ 2^{-J\ \min(m_1,m_2)}. \tag{25}$$

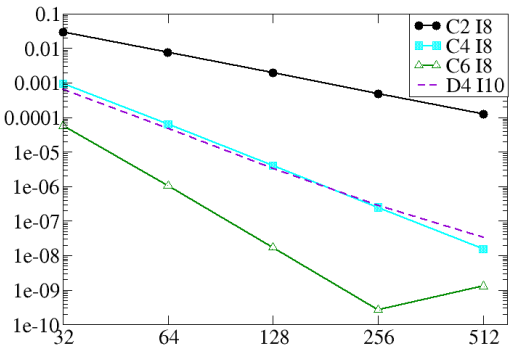

Figure 5: Harmonic Oscillator. Relative error ${}^1\tau_p$ as a function of the resolution 2^J. In three case, $\mathbb{V}_J^{\perp}$ is spanned by Coiflets of order $m_1 = 2, 4, 6$, and in the last one, by a Daubechies basis $D4$.

C2 I8	C4 I8	C6 I8	D4e I10	D4s I8
1.96	3.96	5.86	3.96	3.90

Table 4: Harmonic Oscillator. Convergence rates for the method 1, for different couples (m_1, m_2). s stands for "symmetric", e for "extremal phase".

Table 4 shows the rates corresponding to figure Fig.5. Coiflets are slightly better than Daubechies functions, because the Coiflet scaling functions have vanishing moments.

Method 2 The rates obtained for the relative error in method 2 are relatively high. As observed on figure Fig.6, the error is quadratic:

$$ {}^2\tau_p \sim C_2 \; 2^{-J \min(2m_1, m_2)}, \tag{26} $$

the factor C_2 depending on $||u||_{H^{m_1}}$ and $||u||_{H^{m_2}}$. The energies for the method 2 (Table 5) are of same order as those obtained in the Galerkin formulation (Table 3). We can therefore conclude that this evaluation of the potential energy is optimal: its behavior is as good as the Galerkin one, although its computational complexity is highly reduced.

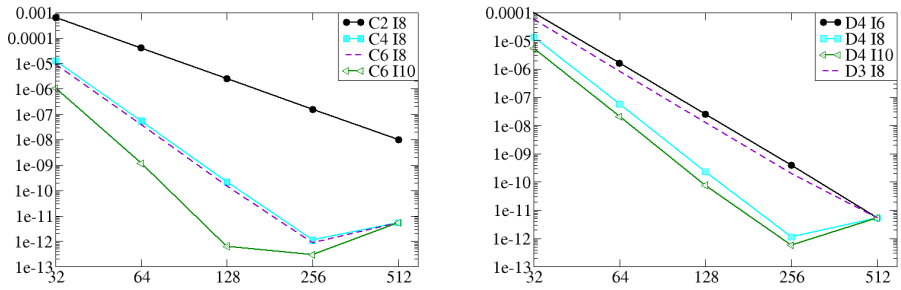

Figure 6: Harmonic Oscillator, ${}^2\tau_p$ as a function of 2^J, for different orthogonal bases m_1: Coiflets (left) and Daubechies (right). The curves $C6I10$ and $D4I10$ show the influence of m_2 on the convergence.

J	D3 I8	D4 I8	C4 I8
5	.750043053	.750010176	.7500094682
6	.75000062740	.750000043524	.750000040569
7	.750000009528	.7500000001122	.75000000010048

Table 5: Harmonic Oscillator. ${}^2\tilde{e}_p$ for different J (column) and different couples $(m_1,\ m_2)$.

4.2 Hydrogen atom

For the Hydrogen atom, the Hamiltonian operator writes $\mathcal{H}_e = -\frac{1}{2}\Delta + V_h$, with $V_h(\mathbf{r}) = -\frac{1}{|\mathbf{r}|}$. The ground state $(\mathcal{E}_h,\ u_h)$ is known analytically:

$$\begin{aligned} u_h(\mathbf{r}) &= C_N\ e^{-|\mathbf{r}|}, \\ e_{kin} &= 0.5\ a.u., \\ e_p &= -1.\ a.u., \end{aligned}$$

where C_N is a normalization constant.

4.2.1 Kinetic energy

The evolution of τ_{kin} depends on the H^s-regularity of the orbital u_h. Indeed, we observe (for instance on figure Fig.7) the following behavior:

$$\tau_{kin} \sim C\ 2^{-2J(\min(m_1,s)-1)},$$

with a prefactor C increasing with m_1. Numerically, the Sobolev regularity of the orbital is around 2.4. This value coincides with a theoretical result obtained by H.-J. Flad (MPI, Leipzig), that would be published, showing that the Hydrogen orbital has a regularity smaller than $\frac{5}{2}$.

On Fig.7, the Daubechies basis behaves slightly better than Coiflets, certainly due to the fact that the Laplacian Stiffness matrix in Daubechies basis is the same that the one in the interpolating basis. For physical systems, where the potential is more irregular, it will be thus not useful to take high order m_1.

4.2.2 Potential Energy

The singularity $\frac{1}{|\mathbf{r}|}$ will be numerically avoided by not centering V_h at a discretisation point.

- At first, we evaluate the relative error when the orbital is the Gaussian u_o. Results of convergence are shown in Table 6. As the singularity does not appear numerically, V_h-regularity does not correspond to the reality. Nevertheless, these convergence rates give information about the quality of the two methods. Actually, it appears that method 2 is in general better that method 1. The values obtained for $C2$ are compatible with the behavior $2^{-J\min(m_1,m_2)}$. The convergence rate is around 4, and certainly represents the numerical regularity of V_h.

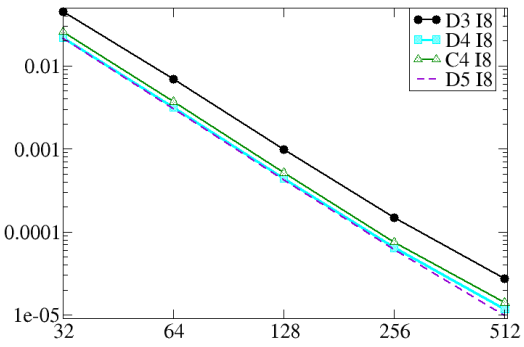

Figure 7: Hydrogen Atom: τ_{kin} as a function of 2^J, for different m_1, m_2.

C2 I6		D3 I6		C4 I6		D4 I6		C6 I8	
2.06	4.05	3.95	4.14	3.97	4.12	3.93	4.06	4.23	4.06

Table 6: Hydrogen Atom with potential V_h and orbital u_o. Convergence rates of relative errors ${}^1\tau_p$ (left) and ${}^2\tau_p$ (right) as a function of (m_1, m_2).

- For the Hydrogen orbital u_h, except for Coiflets of order $m_1 = 2$, we get always a convergence rate between 2.89 and 2.98 for both methods 1 and 2, and for any m_2. In this case, numerical results tend to confirm the estimations (19) and (20). For each couple (m_1, m_2), the error is of order 10^{-4} for $2^J = 128$.

4.2.3 Influence of pseudo-potential

Pseudo-potentials have several properties, the main one being to screen nucleus potential by the first electrons of the atom, to cancel the singularity. In our tests, we use the following one:

$$V_{loc}(\mathbf{r}) = -\frac{1}{|\mathbf{r}|}\mathrm{erf}\left(\frac{|\mathbf{r}|}{\sqrt{2}\,r_{loc}}\right) + e^{-\frac{1}{2}(\frac{|\mathbf{r}|}{r_{loc}})^2}\left(c_1 + c_2(\frac{|\mathbf{r}|}{r_{loc}})^2 + c_3(\frac{|\mathbf{r}|}{r_{loc}})^4 + c_4(\frac{|\mathbf{r}|}{r_{loc}})^6\right),$$

where erf denotes the error function or repartition of the normal law, and C_i, r_{loc} are coefficients depending on atom characteristics. Numerical values

of these parameters can be found in the Physics literature [19]. The second difficulty in atomistic simulations is the long range of potentials, behaving like $1/|\mathbf{r}|$. On the torus Ω, we have to cut it artificially, by applying a window. The Hamiltonian tested here is thus:

$$\mathcal{H} = -\frac{1}{2}\Delta + \widetilde{V} = -\frac{1}{2}\Delta + \frac{V_{loc}(\mathbf{r})}{1 + e^{\beta\ (|\mathbf{r}| - r_c)}}.$$

The orbital u_1 associated to the ground state of the system described by $\mathcal{H}$ is not equal to u_h. Nevertheless we use the couple $(\widetilde{V}, u_h)$ in our numerical tests, knowing that $V(\mathbf{r}) \leqslant \widetilde{V}(\mathbf{r}) \quad \forall\ \mathbf{r} \in \Omega$, implying the energy inequality $e_p \leqslant \dfrac{< u_h\ ,\ \widetilde{V}\ \ u_h >}{< u_h,\ u_h >}$ (recall that e_p is the theoretical Hydrogen potential energy). The ground state orbital u_1 for the potential $\widetilde{V}$ have also to satisfy the same inequality:

$$e_p \leqslant \frac{< u_1\ ,\ \widetilde{V}\ \ u_1 >}{< u_1,\ u_1 >}.$$

Indeed V is deeper than $\widetilde{V}$, meaning that the electron is more attracted by V: this implies that the kinetic energy $\frac{<u_1\ ,\ -\frac{1}{2}\Delta\ u_1>}{<u_1,\ u_1>}$ increases.
Table 7 and Figure Fig.8 show different convergence rates. We get the maximal order 2.95 for $m_1 > 4$ and $m_2 > 4$.

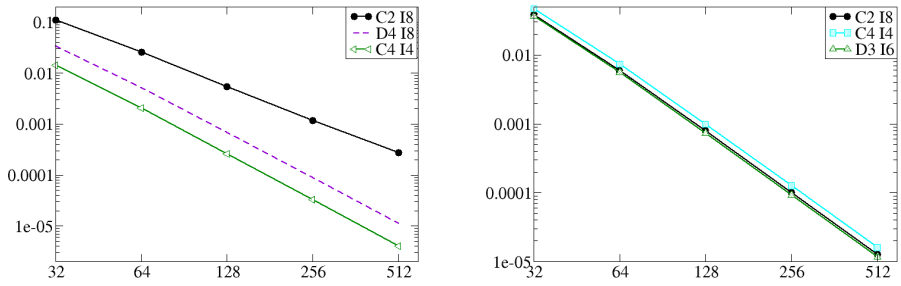

Figure 8: Hydrogen Atom with pseudo-potential. Relative errors (${}^1\tau_p$ (left), and ${}^2\tau_p$ (right)) as a function of 2^J, for several couples (m_1, m_2).

D3 I8	C2 I8	D4 I6	D4 I10	C4 I4	C4 I8	C6 I8
1.9	2.2	2.9	2.9	2.95	2.95	2.95

Table 7: Hydrogen Atom with pseudo-potential. Convergence rates of the relative error ${}^1\tau_p$, for different couples m_1, m_2.

Conclusion

After recalling a priori error estimations for the eigenvalues and the eigenvectors of an elliptic operator, we give error estimations for kinetic and potential energy in specific cases. The approximation is made using Multiresolution Analysis on the tore of $\mathbb{R}^3$. More particularly, we have studied the potential energy, and given different methods to compute this energy to improve the computational cost. These methods are based on the expansion of the potential into an interpolating scaling function basis, whereas the orbitals are expanded into an orthonormal scaling function basis. Their computational costs are optimal, linear in $O(N)$ where N is the dimension of the approximation space, and with a very low prefactor. For both methods, numerical tests on Harmonic Oscillator and on the Hydrogen Atom show their efficiency and accuracy.

Acknowledgements

Authors would like to thank Stefan Goedecker for his first idea to combine different wavelet families in the context of *ab initio* methods. Authors are also indebted to Reinhold Schneider for many fruitful discussions. This work was partially supported by the CEA-Grenoble, and by the IHP network *Breaking Complexity* of the EC (contract number HPRN-CT-2002-00286).

References

[1] T.A. Arias. Multiresolution analysis of electronic structure: semicardinal and orthogonal wavelet bases. *Rev. Mod. Phys.*, 71(1):267–311, 1999.

[2] A.D. Becke. Density-functional exchange-energy approximation with correct asymptotic behaviour. *Phys. Rev. A*, 38(6):3098–3100, 1988.

[3] S. Bertoluzza and G. Naldi. Some remarks on wavelet interpolation. *Comput. Appl. Math.*, 13(1):13–32, 1994.

[4] É. Cancès and C. Le Bris. On the convergence of SCF algorithms for Hartree-Fock equations. *Math. Model. Numer. Anal.*, 34(4):749–774, 2000.

[5] É. Cancès, K. Kudin, G.E. Scuseria, and G. Turinici. Quadratically convergent algorithm for fractional occupation numbers in Density Fonctionnal Theory. *J. Chem. Phys.*, 118(12):5364–5368, 2003.

[6] É. Cancès. *Simulation moléculaire et effets d'environnement. Une perspective mathématique et numérique.* PhD thesis, École Nationale des Ponts et Chaussées, 1998.

[7] C. Chauvin. *Les ondelettes comme fonctions de base dans le calcul de structures électroniques.* PhD thesis, Institut National Polytechnique de Grenoble, 2005.

[8] K. Cho, T.A. Arias, J.D. Joannopoulos, and P. Lam. Wavelets in electronic structure calculations. *Phys. Rev. Lett.*, 71(12):1808–1811, 1993.

[9] A. Cohen. *Numerical Analysis of Wavelet Methods.* North-Holland. Studies in Mathematics and its Application 32, 2003.

[10] W. Dahmen and C. Micchelli. Using the refinement equation for evaluating integrals of wavelets. *SIAM J. Num. Anal.*, 30(2):507–537, 1993.

[11] I. Daubechies. *Ten Lectures on Wavelets.* SIAM, 1992.

[12] R. Dautray and J.-L. Lions. *Analyse mathématique et calcul numérique pour les sciences et techniques: Spectre des opérateurs*, volume 5. Masson, 1988.

[13] G. Deslauriers and S. Dubuc. Symmetric iterative interpolation processes. *Constructive Approximation*, 5(1):49–68, 1989.

[14] T.D. Engeness and T.A. Arias. Multiresolution analysis for efficient, high precision all-electron density-functional calculations. *Phys. Rev. B*, 65(16):165106, 2002.

[15] G.I. Fann, G. Beylkin, R.J. Harrison, and K. Jordan. Singular operators in multiwavelet bases. *IBM J. Res. Dev.*, 48(2):161–171, 2004.

[16] H.-J. Flad, W. Hachbush, D. Kolb, and R. Schneider. Wavelet approximation of correlated wave functions. I Basics. *J. Chem. Phys.*, 116(22):9841–9657, 2002.

[17] S. Goedecker and O.V. Ivanov. Linear scaling solution of the Coulomb problem using wavelets. *Sol. State Commun.*, 105(11):655–669, 1998.

[18] R.J. Harrison, G. Fann, T. Yanai, Z. Gan, and G. Beylkin. Multiresolution quantum chemistry: Basic theory and initial applications. *J. Chem. Phys.*, 121(23):11587–11598, 2004.

[19] C. Hartwigsen, S. Goedecker, and J. Hutter. Relativistic separable dual-space Gaussian pseudo-potentials from H to Rn. *Phys. Rev. B*, 58:3641–3662, 1998.

[20] P. Hohenberg and W. Kohn. Inhomogeneous electron gas. *Phys. Rev. A*, 136(3):B864–B871, 1964.

[21] B.R. Johnson, J.P. Modisette, P. Nordlander, and J.L. Kinsey. Quadrature integration for orthogonal wavelet systems. *J. Chem. Phys.*, 110(17):8309–8317, 1999.

[22] W. Kohn and L.J. Sham. Self-consistent equations including exchange and correlation effects. *Phys. Rev. A*, 140(4):A1133–A1138, 1965.

[23] R.A. Lippert, T.A. Arias, and A. Edelman. Multiscale computation with interpolating wavelets. *J. Comp. Phys.*, 140(2):278–310, 1998.

[24] S. Mallat. *Une exploration des signaux en ondelettes.* Les éditions de l'École Polytechnique, 2000.

[25] D. Marx and J. Hutter. *Ab-initio Molecular Dynamics: Theory and Implementation*, volume 1. Modern Methods and Algorithms of Quantum Chemistry, J. Grotendorst ed., 2000.

[26] A.I. Neelov and S. Goedecker. An efficient numerical quadrature for the calculation of the potential energy of wavefunctions expressed in the daubechies wavelet basis. *J. Comp. Phys.*, 217(2):312 – 339, 2006.

[27] V. Perrier and M.V. Wickerhauser. Multiplication of short wavelet series using connection coefficients. *Advances in Wavelets, K.-S. Lau ed. Springer*, pages 77–101, 1998.

[28] P.-A. Raviart and J.-M. Thomas. *Introduction à l'analyse numérique des équations aux dérivées partielles.* Dunod, 1998.

[29] C.C.J. Roothaan. New developments in molecular orbital theory. *Rev. Mod. Phys.*, 23:69–89, 1951.

[30] R. Schneider and T. Weber. Wavelets for density matrix computation in electronic structure calculation. *Appl. Num. Math.*, 56(10):1383–1396, 2006.

[31] S. Wei and M.Y. Chou. Wavelets in self-consistent electronic structure calculations. *Phys. Rev. Lett.*, 76(15):2650–2653, 1996.

[32] T. Yanai, G.I. Fann, Z. Gan, R.J. Harrison, and G. Beylkin. Multiresolution quantum chemistry in multiwavelet bases: Analytic derivatives for Hartree-Fock and density functionnal theory. *J. Chem. Phys.*, 121(7):2866–2876, 2004.